

DOA Estimation for Low Angle Targets Using Time Reversal in Frequency Domain Model

Xiaolu Zeng*, Baixiao Chen* and Minglei Yang*

Email: feiying3709@sina.com, {bxchen, mlyang}@xidian.edu.cn,

*National Laboratory of Radar Signal Processing, Xidian University, Xi'an, 710071, China

*Collaborative Innovation Center of Information Sensing and Understanding at Xidian University, Xi'an, China

Abstract—Multipath distortion has been a challenge problem for low angle target localization problem using very high frequency (VHF) radar. In particular, under complex terrain, part of the multipath lies in the same beamwidth of the direct path signal, which makes it difficult to be distinguished in the spatial, temporal and Doppler domains. This paper uses time reversal (TR) technique to adjust the transmitting signal waveform by exploring the channel information contained in multipath clutters. According to TR principle, this specially designed signal can refocus at the original target position, which not only mitigates the multipath distortion but also equally increases the signal-to-noise ratio (SNR) of the TR receiving signal. Next, we analyze the independence between the noise subspace and the sampling frequency bin in our TR wideband signal model. A novel direction of arrival (DOA) estimation method is then investigated in frequency domain. Compared with conventional methods, its superiority in DOA estimation accuracy for low angle targets is validated by numerical simulations.

I. INTRODUCTION

Very high-frequency (VHF) radar system is often used for low-angle target detection and localization because of its advantages in anti-stealth, anti-anti radiation missile property [1], [2]. Moreover, multipath distortion is an inevitable headache in this localization system especially under complex terrain with rich scatters [2]. Generally, researchers try to utilize channel equalization or filtering techniques to eliminate (or mitigate more practically) the negative effect of multipath signals. However, in complex terrain, multipath signals are stochastically distributed and thus difficult to be distinguished from the direct path signal. As a result, most direct-path based DOA estimation methods degrade seriously or even fail. Is multipath signal always detrimental or can we make use of the information contained in multipath signal to improve the DOA estimation performance? Fortunately, time reversal (TR) technique answers this question positively in recent years.

TR technique was firstly studied to compensate the phase-delay distortion during long-distance transmissions over telephone lines [3]. Until 1992, in a practical underwater experiment, M. Fink and his research team observed that the energy of the TR acoustic signal from transmitter could refocus at an intended location with very high spatial resolution [4]. However, TR spatial focusing calls for large bandwidth and high sample rate to harvest enough large number of multipaths, which is difficult or impossible in the past. With the development of modern radio frequency devices and semiconductors, TR in the electromagnetic domain has begun to become a viable approach. Thus, it is being widely studied such as in acoustics [5] and wireless networks [6]. In radar

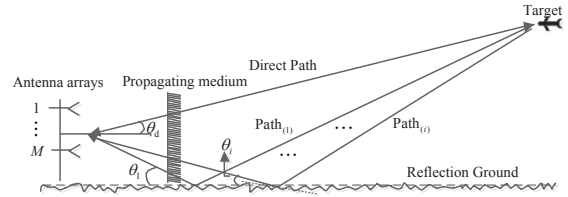


Fig. 1. Geometry of reflection for the TR DOA estimator.

systems, related researches include TR-based wideband Capon algorithms [7], TR-MIMO radar system [8], TR-CS/MIMO [9], TR-MUSIC methods [10] and so on.

In this paper, we investigate a new DOA estimation method in frequency domain for low angle targets which is termed as time reversal noise subspace based spatial smoothing MUSIC (TRNSB-SSMUSIC). Compared with the conventional methods, TRNSB-SSMUSIC firstly designs the TR transmitting signal by time-reversing (equal to phase conjugation and energy normalization in frequency domain) the received signals. Then, an extra TR setup is added to re-transmit the TR transmitting signal back to the target. The backscattered signals in the TR setup are then used for DOA estimation. By using TR technique, the TR transmitting waveform can inherently match the propagation channel and refocus at the original source location to increase the signal-to-noise ratio (SNR). Moreover, wideband TR transmitting signal is taken here to harvest enough multipath information, which then causes wideband observed data. However, in wide-band localization signal processing, angular frequency ω is a variable parameter, which cause the ambiguity in (ω, θ) pairs. To solve this problem, we employ an additional independent temporally delayed sampling at the outputs of the arrays [11]. Therefore, sources of different temporal frequencies are further separated in angle and can be more easily distinguished. We then analyze the independence of the noise subspace versus different frequency bins and develops a noise subspace based DOA estimation method. Compared with traditional coherent signal processing method, TRNSB-SSMUSIC shows better DOA estimation potential because it does not need preliminary DOAs. Numerical simulations indicate that our TRNSB-SSMUSIC outperforms conventional methods in DOA estimation accuracy for low angle target with rich multipath distortion under complex terrain.

II. SIGNAL MODEL

As shown in Fig. 1, we consider a uniform linear array (ULA) with M elements and a low angle target with P signals

scattered back by the target and reflection ground into the array. For typical VHF radar systems, the range between the target and the antenna is far enough so that a far field approximation holds. The array firstly transmits a known complex bandpass probing signal $f(t)e^{jw_c t}$ with w_c denoting the angular carrier frequency. The receiving signal at the m th element is given by

$$r_m(t) = \sum_{p=1}^P X_p f(t - \tau_{(p,1)} - \Delta\tau_{(1,m,p)}) + v_m(t), \quad (1)$$

where $t = t_1, t_2, \dots, t_N$ and N is the number of snapshots. X_p , $\tau_{(p,1)}$ and $\Delta\tau_{(k,p)}$ respectively denote the attenuation factor, reference propagation delay and inter-element delay of corresponding path p . $v_m(t)$ represents the additive Gaussian noise factor. Then, after Fast Fourier Transformation (FFT), we can rewrite (1) in frequency domain as

$$R_m(\omega) = \sum_{p=1}^P X_p F(\omega) e^{-j\omega\tau_{(p,1)}} e^{-j\omega\Delta\tau_{(1,m,p)}} + V_m(\omega), \quad (2)$$

where $R_m(\omega)$, $F(\omega)$ and $V_m(\omega)$ are the FFT forms of $r_m(t)$, $f(t)$ and $v_m(t)$, respectively. By synthesizing the observed data of all the M elements into a vector, we obtain

$$\mathbf{y}(\omega) = \mathbf{A}(\Theta, \omega) \mathbf{X} \Gamma(\omega) \mathbf{F}(\omega) + \mathbf{v}(\omega), \quad (3)$$

where $\mathbf{y}(\omega)$ is called Forward-Echo to be distinguished from the TR-Echo in the TR probing setup. In (3),

$$\begin{aligned} \Theta &= [\theta_1, \dots, \theta_P], \mathbf{A}(\Theta, \omega) = [\mathbf{a}(\theta_1, \omega), \dots, \mathbf{a}(\theta_P, \omega)], \\ \mathbf{a}(\theta_p, \omega) &= [1, e^{-j\omega d \sin \theta_p / c}, \dots, e^{-j(M-1)\omega d \sin \theta_p / c}]^T, \quad (4) \\ \mathbf{X} &= \text{diag}\{x_1, \dots, x_P\}, \Gamma(\omega) = [e^{-j\omega\tau_1}, \dots, e^{-j\omega\tau_P}]^T, \end{aligned}$$

where d and c represent the inter-element space and signal propagation speed. Symbol $\text{diag}\{\mathbf{x}\}$ generates a square matrix with elements of \mathbf{x} on the main diagonal. $\mathbf{A}(\Theta, \omega)$ and $\mathbf{F}(\omega)$ are steering matrix and signal vector. \mathbf{X} and $\Gamma(\omega)$ denote path attenuation matrix and propagation delay vector, respectively. It is noted that the inter-element delay of path p is given by $\Delta\tau_{(1,m,p)} = (m-1)d \sin \theta_p / c$ in array signal processing.

Next, we design the TR transmitting signal $F_{\text{TR}}(\omega)$ by digitizing, time-reversing and energy normalizing the Forward-Echo $\mathbf{y}(\omega)$. g is the energy normalization factor.

$$F_{\text{TR}}(\omega) = g \mathbf{y}^*(\omega), \quad g = \sqrt{(\|\mathbf{F}(\omega)\|^2) / (\|\mathbf{y}(\omega)\|^2)}, \quad (5)$$

Then, $F_{\text{TR}}(\omega)$ is retransmitted back into the probing environment to detect the target again. If the reciprocity of the propagation medium strictly holds (actually most TR based methods assume so such as [7], [12]), $F_{\text{TR}}(\omega)$ will undergo similar changes, which may include multipath scattering, propagation attenuation and refraction, as that of the forward probing signal $F(\omega)$ and finally be recorded by the array. The receiving signal in this TR setup is named as TR-Echo $\mathbf{y}_{\text{TR}}(\omega)$, which is given by (6) from simple analogy to (3).

$$\mathbf{y}_{\text{TR}}(\omega) = \sum_{m=1}^M \mathbf{A}(\Theta, \omega) \mathbf{X} \Gamma(\omega) F_{\text{TR}}^m(\omega) + \mathbf{n}(\omega). \quad (6)$$

In (6), $F_{\text{TR}}^m(\omega)$ denotes the m th entry of $F_{\text{TR}}(\omega)$ and $\mathbf{n}(\omega)$ represents the Gaussian noise brought in during TR probing

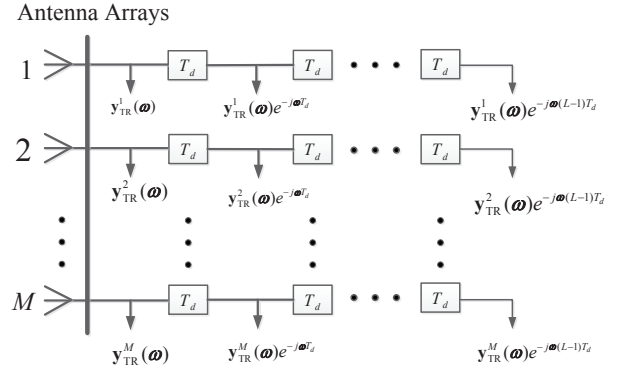


Fig. 2. Geometric implementation of the inserting temporally delay scheme.

process. (6) can be given in a more compact matrix form as

$$\begin{aligned} \mathbf{y}_{\text{TR}}(\omega) &= \mathbf{A}(\Theta, \omega) \mathbf{X} \Gamma_{\text{TR}}(\omega) F_{\text{TR}}(\omega) + \mathbf{n}(\omega) \\ &= \mathbf{A}(\Theta, \omega) \mathbf{S}_{\text{TR}}(\omega) + \mathbf{n}(\omega). \end{aligned} \quad (7)$$

where $\Gamma_{\text{TR}}(\omega) = [\Gamma(\omega)] \cdots [\Gamma(\omega)]_{P \times M}$ and $\mathbf{S}_{\text{TR}}(\omega) = \mathbf{X} \Gamma_{\text{TR}}(\omega) F_{\text{TR}}(\omega)$ representing the TR source signal.

III. THE PROPOSED TRNSB-SSMUSIC ALGORITHM

In this section, we firstly analyze and solve the ambiguity problem in the (ω, θ) pairs. Then, our TRNSB-SSMUSIC algorithm is derived from the TR-Echo given in (7).

A. Ambiguity in (ω, θ) pairs

In broadband source localization signal processing, the steering vector $\mathbf{a}(\theta, \omega)$ in (4) is a function of $\omega \cdot \sin \theta$. Thus, all (ω, θ) pairs in which $\omega \cdot \sin \theta$ equals with a same number will cause an ambiguous set since their M -dimensional steering vectors are equivalent. In this case, we consider to introduce an extra time delay vector independent with angle θ at the outputs of the array to eliminate the ambiguity [11]. Fig. 2 shows the scheme of the time delay vector $\mathbf{D}(T_d)$ inserted into the original output observations.

$$\mathbf{D}(T_d) = [1, e^{-j\omega T_d}, \dots, e^{-j\omega(L-1)T_d}]^T, \quad (8)$$

In (8), T_d is the inserted sample delay. By employing this L order temporally delay, the new steering vector $\mathbf{a}^{\text{D}}(\theta, \omega)$ and output observed data $\mathbf{y}_{\text{TR}}^{\text{D}}(\omega)$ can be expressed as :

$$\begin{aligned} \mathbf{a}^{\text{D}}(\theta, \omega) &= \mathbf{a}(\theta, \omega) \otimes \mathbf{D}(T_d) \\ \mathbf{y}_{\text{TR}}^{\text{D}}(\omega) &= \mathbf{y}_{\text{TR}}(\omega) \otimes \mathbf{D}(T_d), \end{aligned} \quad (9)$$

where \otimes is Kronecker product. By this transformation, $\mathbf{a}^{\text{D}}(\theta, \omega)$ becomes a monochromatic function of (ω, θ) pair and avoid the ambiguity between ω and θ effectively. Note that there are two marks here. First, for $l \in \{1, \dots, L-1\}$, t_d should be strictly selected so that $l\omega T_d \bmod 2\pi$ is unambiguous over $\omega \in \Omega$, where Ω is the signal band. Otherwise, new ambiguous will be induced. Second, in particular numerical methods, the ambiguous (ω, θ) pair may not lie in the interested band Ω of angle space Θ . Therefore, we do not need to this time delay insertion since the M -dimensional steering vectors are unique and these ambiguous (ω, θ) pairs do not affect our DOA estimation results. In this case, $\mathbf{y}_{\text{TR}}(\omega)$ and $\mathbf{A}(\Theta, \omega_q)$ we will use in the rest of the paper have eliminated

the ambiguity between ω and θ if it is necessary. To simplify notation, we omit the superscript $\mathbf{y}_{\text{TR}}^{\text{D}}(\omega)$ and $\mathbf{A}^{\text{D}}(\Theta, \omega_{\mathbf{q}})$.

B. TRNSB-SSMUSIC Algorithm

Next, we derive our TRNSB-SSMUSIC algorithm on the base of the TR-Echo $\mathbf{y}_{\text{TR}}(\omega)$. Firstly, $\mathbf{y}_{\text{TR}}(\omega)$ is uniformly divided into Q frequency bins. Then, for a fixed frequency ω_q , the corresponding covariance matrix $\mathfrak{R}_{\mathbf{y}}^{\text{TR}}(\omega_q)$ can be computed by

$$\begin{aligned} \mathfrak{R}_{\mathbf{y}}^{\text{TR}}(\omega_q) &= \mathbb{E} \left\{ \mathbf{y}_{\text{TR}}(\omega_q) \mathbf{y}_{\text{TR}}(\omega_q)^H \right\} \\ &= \mathbf{A}(\Theta, \omega_q) \mathfrak{R}_{\text{TR}}(\omega_q) \mathbf{A}^H(\Theta, \omega_q) + \mathfrak{R}_{\text{N}}(\omega_q), \end{aligned} \quad (10)$$

where \mathbb{E} represents expectation operator. $\mathfrak{R}_{\text{TR}}(\omega_q)$ and $\mathfrak{R}_{\text{N}}(\omega_q)$ denote the covariance matrix of the TR source signal $\mathbf{S}_{\text{TR}}(\omega_q)$ and noise $\mathbf{n}(\omega_q)$, respectively. Evidently, signal subspace is closely related with frequency ω_q because it can be equally spanned by the columns of $\mathbf{A}(\Theta, \omega_q)$. However, for noise subspace, we can obtain that $\mathfrak{R}_{\text{nn}}(\omega_q) = \sigma^2 \mathbf{I}$, where σ^2 denotes the power spectral density of the noise $\mathbf{n}(\omega_q)$ and \mathbf{I} is the identity matrix of order M . It is easy to see that $\mathfrak{R}_{\text{nn}}(\omega_q)$ is not related with frequency bin ω_q if $\mathbf{n}(\omega_q)$ is assumed to be an additive Gaussian noise, which is reasonable in practice. Then, (10) can be rewritten as

$$\mathfrak{R}_{\mathbf{y}}^{\text{TR}}(\omega_q) = \mathbf{A}(\Theta, \omega_q) \mathfrak{R}_{\text{TR}}(\omega_q) \mathbf{A}^H(\Theta, \omega_q) + \sigma^2 \mathbf{I}, \quad (11)$$

For wideband source localization signal processing, the average covariance matrix in frequency domain is given by

$$\mathfrak{R}_{\mathbf{y}}^{\text{TR}}(\omega) = \frac{1}{Q} \sum_{q=1}^Q \mathbf{A}(\Theta, \omega_q) \mathfrak{R}_{\text{TR}}(\omega_q) \mathbf{A}^H(\Theta, \omega_q) + \sigma^2 \mathbf{I} \quad (12)$$

From (12), it is clear that the noise subspace of $\mathfrak{R}_{\mathbf{y}}^{\text{TR}}(\omega)$, which is equivalent to the space spanned by the eigenvectors of $\sigma^2 \mathbf{I}$, is independent with frequency ω .

In low angle scenario, most multipaths are coherent with the direct path signal. Especially, in wideband array signal processing, multipath components and direct path signal can be treated as coherent sources if $|\tau_{(p_1,1)} - \tau_{(p_2,1)}| \leq \tau_R$ holds [13]. Note that $p_1, p_2 = 1, 2, \dots, P$ with $p_1 \neq p_2$ and $\tau_R = 1/B$, where B is the bandwidth of the probing signal. Considering this reason, $\mathfrak{R}_{\text{TR}}(\omega)$ is a singular matrix in most low angle cases or an approximate singular matrix because the signal subspace will expand into the noise subspace in some cases. Signal subspace expansion is also a typical problem in wideband source localization signal processing, about which readers can refer to [14] for details. In other words, $\mathfrak{R}_{\text{TR}}(\omega)$ cannot be directly used to separate coherent sources by using eigen subspace decomposition methods such as typical MUSIC. To solve this problem, spatial smoothing (SS) technique [15] is used here to recover the rank of $\mathfrak{R}_{\text{TR}}(\omega)$. Also, we omit the detailed process about the SS technique for notation simplicity. We denote the average covariance matrix after SS processing as $\mathfrak{R}_{\mathbf{y}}^{\text{TRSS}}(\omega)$. Then, the pseudo-spectrum of our proposed TRNSB-SSMUSIC algorithm can be derived as

$$\mathbb{P}_{\text{TR}}(\theta) = \frac{1}{Q} \sum_{q=1}^Q \frac{1}{\mathbf{a}^H(\theta, \omega_q)(\theta) \hat{\mathbf{U}}_N \hat{\mathbf{U}}_N^H \mathbf{a}(\theta, \omega_q)}, \quad (13)$$

TABLE I. PARAMETERS USED IN THE MONTE CARLO SIMULATIONS

Number of frequency bins Q		30
Direct path time delay		$\tau_{(p,1)} = 2\text{ms}$
2-path	True direction of arrival	$\{2^\circ, -2^\circ\}$
	Time delays	$\{0, 2\}\text{ns}$
	Attenuation factors	$\{1, 0.9\}$
3-path	True direction of arrival	$\{2^\circ, -2^\circ, -10^\circ\}$
	Time delays	$\{0, 2, 10\}\text{ns}$
	Attenuation factors	$\{1, 0.9, 0.3\}$
4-path	True direction of arrival	$\{2^\circ, -2^\circ, -10^\circ, -20^\circ\}$
	Time delays	$\{0, 2, 10, 20\}\text{ns}$
	Attenuation factors	$\{1, 0.9, 0.3, 0.16\}$

where θ is the search angle, $\mathbf{a}^H(\theta, \omega_q)$ is the steering vector as defined in (4). $\hat{\mathbf{U}}_N$ is the noise subspace which can be obtained from the eigen-decomposition of $\mathfrak{R}_{\mathbf{y}}^{\text{TRSS}}(\omega)$.

IV. NUMERICAL SIMULATIONS

In this section, we take numerical experiments to evaluate the DOA estimation performance of the proposed TRNSB-SSMUSIC algorithm introduced in Section II and III. In all simulations, we mainly compare it with three benchmark algorithms. Specifically, in Fig. 3 and Fig. 4, CNSB-SSMUSIC represents an conventional algorithm using the same noise subspace principle with our TRNSB-SSMUSIC except that it does not take TR technique to deal with multipath. It is mainly to test the efficiency of our using TR technique to mitigate multipath distortions. On the other hand, C-RSSFocus and TR-RSSFocus denote two methods using coherent signal subspace method (CSSM) to deal with the wideband source signals. Note that CSSM is a typical kind of coherent wideband signal processing methods by focusing the wideband observations into one predefined frequency bin. Herein, we take the coherent signal rotational subspace (RSS) [16] focusing technique as an example to verify the rationality of our noise subspace based method in processing wideband receiving signals. Corresponding method which does not take or jointly utilizes TR technique are named as C-RSSFocus and TR-RSSFocus, respectively. Mainly, two numerical simulations are shown to verify the proposed algorithm: i) the spatial spectra; ii) root mean squares errors (RMSE) with respect to different SNRs by the Monte Carlo simulations. In addition, we analyze the computational complexity of our method and compare it with other three algorithms. Its advantage and disadvantage in complexity are clearly stated at last.

All the experiments are conducted on the base of the a ULA containing 16 isotropic elements as shown in Fig. 1. The inner element space is $d = \lambda_0$ with $\lambda_0 = c/f_c$, where f_c is the carrier frequency and c is the propagation speed of the probing signal. Moreover, the probing signal is a pulse with linear frequency modulation (LFM) with $f_c = 200\text{MHz}$, which is commonly used in VHF radar systems. The bandwidth is $B = 20\text{MHz}$ and equally sampled into 30 frequency bins. Other parameters including true DOAs, time delays and attenuations factors under different number of multipath scenarios are listed in Table I. Note that the time delays are computed with the direct path time delay as the reference propagation delay.

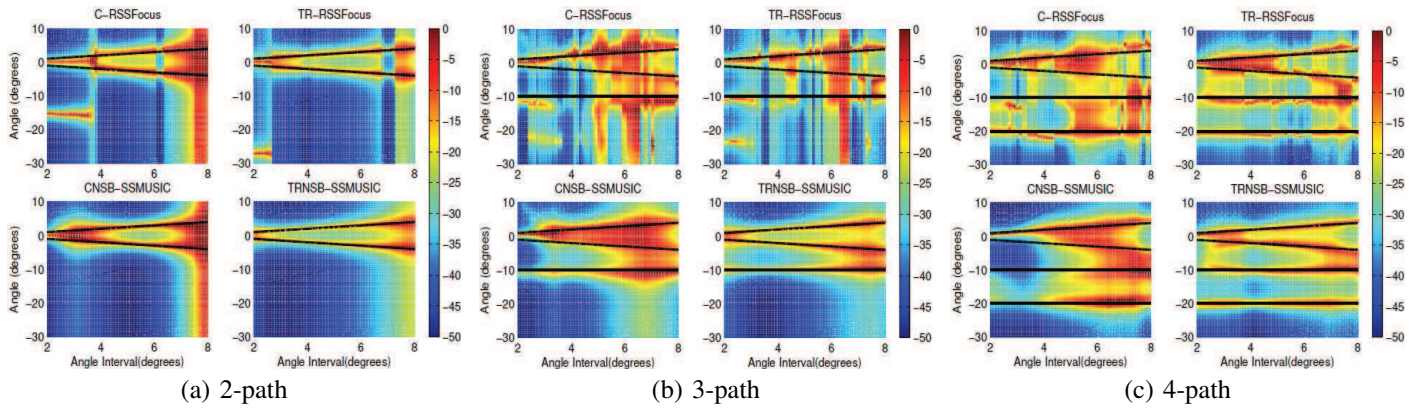


Fig. 3. Spectra of the four different algorithms versus different angle intervals between the direct path and adjacent multipath: (a)2-path; (b)3-path; (c)4-path.

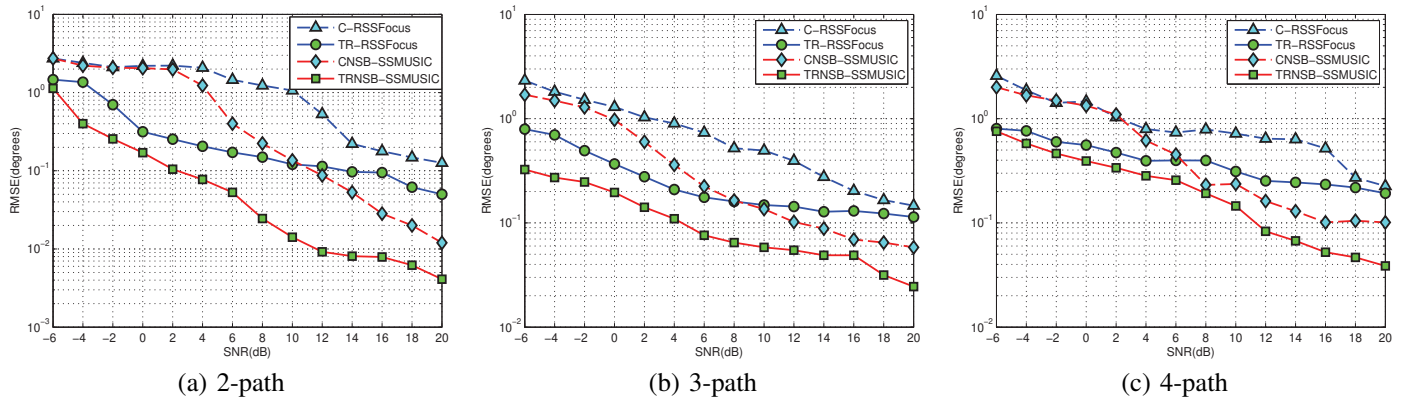


Fig. 4. RMSE performance curves of the four algorithms in different propagation models: (a)2-path; (b)3-path; (c)4-path.

A. Spatial Spectra

Fig. 3 depicts the normalized spectra of the four different algorithms in different 2-, 3- and 4-path models. SNRs in Fig. 3 are fixed at 10 dB for all of the three propagation models. For easy reference, in Fig. 3, several solid lines are plotted to mark the actual DOAs. Moreover, in order to test the angle resolution simultaneously, we change the angle intervals between the direct path and the adjacent multipath from 2° to 8° . This adjacent multipath signal is also called the major specular reflection signal in low angle scenario. Furthermore, it is often treated as a symmetrical signal of the direct path signal with the reflection ground working as the symmetrical plane. Here, we take these research results by setting the angle of direct path from 1° to 4° and the angle of adjacent multipath symmetrically. For multipath signals far away from the direct path signal (mainly reflected from the diffuse reflection area actually), we set them in different beamwidths with the direct path signal, which is reasonable in practice.

Fig. 3 depicts that in all of three propagation models, our TRNSB-SSMUSIC shows better resolution performance than other three methods. Specifically, Table II lists the smallest angle interval between the direct path and adjacent multipath which can be resolved successfully. Here, we take the resolution definition as in [17]. If $\mathbb{P}[(\theta_1 + \theta_1)/2] \leq [\mathbb{P}(\theta_2) + \mathbb{P}(\theta_2)]/2$, then θ_1 and θ_2 are resolved successfully, where θ_1 and θ_2 represents two adjacent peaks in the pseudo-spectrum of corresponding algorithms. In all of the scenarios

TABLE II. SMALLEST SUCCESSFUL RESOLVED ANGLE INTERVAL OF DIFFERENT ALGORITHMS IN DIFFERENT PROPAGATION MODELS

Path	Fig.No	DOA Method			
		C-RSSFoc	TR-RSSFoc	CNSB-SSMUSIC	TRNSB-SSMUSIC
2	3.(a)	3.8°	2.6°	2.6°	2°
3	3.(b)	5.4°	3.8°	3.2°	2.4°
4	3.(c)	6.2°	4.4°	5°	3.2°

shown in Fig. 3, C-RSSFoc and TR-RSSFoc suffer from fake peaks in some extent. The reason is that RSS based wideband source localization algorithms heavily depend on the accuracy of preliminary DOAs, which is very difficult for low angle targets under complex terrain especially at low SNRs. By respectively comparing C-RSSFoc with TR-RSSFoc and CNSB-SSMUSIC with TRNSB-SSMUSIC, we can easily conclude that algorithms which jointly take TR technique show better performance. This superiority benefits from the TR technique which designs a special transmitting signal which can match the channel automatically and refocus at the target position. In other words, this TR process improves the SNRs and generates a larger virtual aperture, thus resulting better DOA estimation results.

B. RMSE versus SNRs

In Fig. 4, we mainly compare the DOA estimation accuracy of the four algorithms in terms of RMSE versus different SNRs. Note that these results are based on 1000 Monte Carlo

TABLE III. COMPUTATIONAL COMPLEXITY COMPARISONS

Algorithms	Computational complexity	$L = 1$	$L = 2$
C-RSSFocus	$O\{M[\frac{N}{2}\log_2(N)] + 3QM^3 + (2QP + 14J)M^2 + JQ(M^2 + M)\}$	4.801×10^7	4.801×10^7
TR-RSSFocus	$O\{3M[\frac{N}{2}\log_2(N)] + 4MN + 3QM^3 + (2QP + 14J)M^2 + JQ(M^2 + M)\}$	4.931×10^7	4.931×10^7
CNSB-SSMUSIC	$O\{M[\frac{N}{2}\log_2(N)] + L^2M^2(Q + LM) + JLM[2(M - P) + 1]\}$	3.275×10^6	1.237×10^7
TRNSB-SSMUSIC	$O\{3M[\frac{N}{2}\log_2(N)] + 4MN + L^2M^2(Q + LM) + JLM[2(M - P) + 1]\}$	4.259×10^6	1.335×10^7

simulations using the parameters listed in Table I. Clearly, the proposed TRNSB-SSMUSIC method shows lower RMSE values than other three algorithms, which indicates that it improves the DOA estimation accuracy in a certain degree.

C. Computational Complexity Analysis

In this subsection, we analyze the computational complexity of our TRNSB-SSMUSIC algorithm and compare it with other benchmark algorithms. The entire DOA estimation process can be divided into several steps. One time of complex multiplication (CM) is taken as the unit of complexity.

- 1) FFT transformation takes $M[\frac{N}{2}\log_2(N)]$ CMs.
- 2) Time reversal process takes $O(4MN)$ CMs.
- 3) Covariance matrix $\mathfrak{R}_y^{\text{TR}}(\omega_q)$ takes $O[Q(LM)^2]$ CMs.
- 4) Eigenvalue decomposition takes $O[(LM)^3]$ CMs.

5) Estimation of $\mathbb{P}_{TR}(\theta)$ takes $O\{LM[2(LM - P) + 1] \cdot J\}$ CMs, where J denotes the angle grid number, i.e., $\{\theta_b\}_{j=1}^J$ covers the all the possible directions of θ .

Table III summarizes the overall computational complexity of the four algorithms. It can be easily concluded that our new methods takes lower computational complexity. This can be obtained from (13) that the new methods just takes one time eigenvalue decomposition while the RSS based method should conduct eigenvalue decomposition at every frequency bin and compute corresponding focusing matrix. However, it should be remarked that with L increasing, the complexity of our method increase quickly because the dimension of the covariance matrix is directly related with L . As a result, corresponding eigenvalue decomposition will take much more computational complexities. A reasonable way is to analyze the ambiguity problem first as Section III.A described and then select proper L if it is necessary. Readers should balance the computational load and accuracy enhancement in practice.

V. CONCLUSION

This paper proposes a novel time reversal based DOA estimation method for low angle target localization problems. The transmitting signal designed by TR can match the multipath channel well and lead to better estimation performance. Moreover, the ambiguity problem between angle and frequency in wideband signal process is solved by an independent time delay method. Third, in frequency domain, the noise subspace is proved to be independent with the frequency bins. Therefore, it can be used for wideband source localization directly, thus, reducing the the computational load. Numerical simulations validate that the proposed algorithm has better DOA estimation accuracy, resolution and exhibits lower RMSE than other three methods. Furthermore, TR transmitting signal is assumed to match the propagation channel perfectly in this paper. In practice, many factors such as the noise will lead

to channel estimation errors and degrade the DOA estimation performance. Hence, corresponding DOA estimation methods with channel mismatch is worthy to be further studied.

ACKNOWLEDGMENT

This work is supported by the Natural Science Foundation of China (No. 61571344).

REFERENCES

- [1] Z. Xu, Z. Xiong, J. Wu, and S. Xiao, "Symmetrical difference pattern monopulse for low-angle tracking with array radar," *IEEE Transactions on Aerospace and Electronic Systems*, vol. 52, no. 6, pp. 2676–2684, December 2016.
- [2] B. Chen, G. Zhao, and S. Zhang, "Altitude measurement based on beam split and frequency diversity in VHF radar," *IEEE Transactions on Aerospace and Electronic Systems*, vol. 46, no. 1, pp. 3–13, Jan 2010.
- [3] B. Bogert, "Demonstration of delay distortion correction by time-reversal techniques," *IRE Transactions on Communications Systems*, vol. 5, no. 3, pp. 2–7, December 1957.
- [4] M. Fink, "Time reversal of ultrasonic fields. i. basic principles," *IEEE Transactions on Ultrasonics, Ferroelectrics, and Frequency Control*, vol. 39, no. 5, pp. 555–566, Sept 1992.
- [5] M. Fink and C. Prada, "Acoustic time-reversal mirrors," *Inverse Problems*, vol. 17, no. 1, 2001.
- [6] K. J. R. Liu, B. Wang, Y. Han, H. Q. Lai, and Z. Safar, "Why time reversal for future 5G wireless?" *IEEE Signal Processing Magazine*, vol. 33, no. 2, pp. 17–26, March 2016.
- [7] F. Foroozan and A. Asif, "Time reversal based active array source localization," *IEEE Transactions on Signal Processing*, vol. 59, no. 6, pp. 2655–2668, June 2011.
- [8] F. Foroozan, A. Asif, and Y. Jin, "Cramer-rao bounds for time reversal mimo radars with multipath," *IEEE Transactions on Aerospace and Electronic Systems*, vol. 52, no. 1, pp. 137–154, February 2016.
- [9] M. H. S. Sajjadih and A. Asif, "Compressive sensing time reversal mimo radar: Joint direction and doppler frequency estimation," *IEEE Signal Processing Letters*, vol. 22, no. 9, pp. 1283–1287, Sept 2015.
- [10] D. Ciuonzo and P. S. Rossi, "Noncolocated time-reversal music: High-rank distribution of null spectrum," *IEEE Signal Processing Letters*, vol. 24, no. 4, pp. 397–401, 2017.
- [11] K. M. Buckley and L. J. Griffiths, "Broad-band signal-subspace spatial-spectrum (bass-ale) estimation," *IEEE Transactions on Acoustics, Speech, and Signal Processing*, vol. 36, no. 7, pp. 953–964, Jul 1988.
- [12] X. Zeng, M. Yang, B. Chen, and Y. Jin, "Low angle direction of arrival estimation by time reversal," in *2017 IEEE International Conference on Acoustics, Speech and Signal Processing (ICASSP)*, March 2017, pp. 3161–3165.
- [13] R. A. Monzingo, R. L. Haupt, and T. W. Miller, *Optimum Array Processing*. IET Digital Library, 2011.
- [14] J. Hudson, *Adaptive array principles*. IET, 1981, vol. 11.
- [15] T. Shan, M. Wax, and T. Kailath, "On spatial smoothing for direction-of-arrival estimation of coherent signals," *IEEE Transactions on Acoustics, Speech, and Signal Processing*, vol. 33, no. 4, pp. 806–811, Aug 1985.
- [16] H. Hung and M. Kaveh, "Focussing matrices for coherent signal-subspace processing," *IEEE Transactions on Acoustics, Speech, and Signal Processing*, vol. 36, no. 8, pp. 1272–1281, Aug 1988.
- [17] Y. Wang and H. Chen, *Spectra Estimation Theory and Algorithm*. Tsinghua University Press, 2009.